THE JOURNAL OF PHYSICAL CHEMISTRY B

Article

pubs.acs.org/JPCB

Chain Length Dependent Excited-State Decay Processes of Diluted PF2/6 Solutions

João Pina,[†] J. Sérgio Seixas de Melo,*[,†] Niels Koenen,[‡] and Ulli Scherf[‡]

[†]Department of Chemistry, University of Coimbra, Rua Larga, 3004-535 Coimbra, Portugal

[‡]Makromolekulare Chemie, Bergische Universität Wuppertal, Gaußtraße 20, 42097 Wuppertal, Germany

Supporting Information

ABSTRACT: The excited-state dynamics of a series of four poly[2,7-(9,9-bis(2-ethylhexyl)fluorene] fractions, PF2/6, with different chain length (degrees of polymerization DP: 5, 10, 39, and 205) was investigated in dilute solutions by steady-state and time-resolved fluorescence techniques. Two decay components are extracted from time-resolved fluorescence experiments in the picosecond time domain: a chain length dependent, fast decay time (τ_2) for shorter emission wavelengths (ranging from 30 to 41 ps), which is associated with a rising component at longer wavelengths, and a longer decay time, τ_1 (ranging from 387 to 452 ps). The system was investigated with kinetic formalisms involving (i) a two-state system (A and B) involving conformational relaxation of the initially excited PF2/6 segment (A) under formation of a more planar (B) relaxed state and (ii) a time-dependent red shift of the emission spectrum using the Stokes shift correlation function (SSCF). In the case of (i), the kinetic scheme was solved considering the simultaneous excitation of A and B or only of A, and the rate constants for formation [k'_{CR} or $k'_{CR}(\alpha)$], dissociation (k_{-CR}), and deactivation (k_B^*) were obtained together with the fraction of species A and B present in the ground state. The use of the SSCF in (ii) was found to be more adequate leading to a decay law with a 3.4 ps component (associated with the slow part of the solvation dynamics process) and a longer decay (43.3 ps) associated with the conformational/torsional relaxation process with a rate constant k_{CR}. This longer component of the SSCF was found to be identical to the short-living decay (τ_2) component of the biexponential decays, displaying an Arrhenius-type behavior with activation energy values in the range 5.8−8.9 kJ mol^{-1} in toluene and 6.5−10.7 kJ mol^{-1} in decalin. From the dependence of the fast decay component ($k_{CR} \equiv 1/\tau_2$) on solvent viscosity and temperature, the activation energy for the conformational relaxation process was found to be distinctly dependent on the chain length, with the relaxation rate dependence with the solvent viscosity ($k_{CR} \approx \eta^{-\gamma}$) displaying $\gamma = 1$ for the oligomer fraction with DP = 5 (i.e., k_{CR} is associated with a pure diffusion-controlled process) and $\gamma < 1$ for the higher molecular weight PF2/6 fractions (with DP = 10, 39, 205). This happens because of a decreased conformational barrier between nonrelaxed and relaxed states promoted by the polymer skeleton.

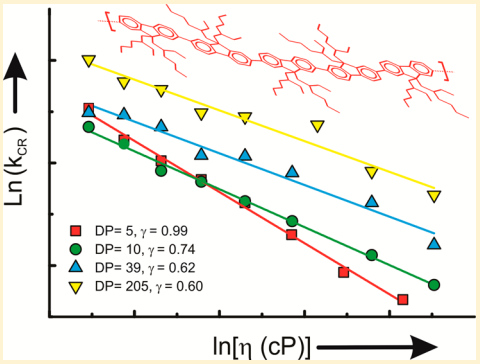

INTRODUCTION

The study of conjugated polymers (CPs), which can be considered as multichromophoric systems with the number of chromophores strongly depending on the chain length, and in particular the investigation of isolated CP chains with emphasis on the excited-state decay processes occurring in these systems, have attracted much attention over the past 2 decades.[1−7] Tuning of the photophysical properties of CPs has led to the development of new functional materials for optoelectronic applications.[8−15] Whereas in small π-conjugated organic molecules the excited state is often extended across the whole molecule, the situation in conjugated polymers is more complex. In CPs, the excitons are delocalized over a restricted range (the so-called effectively conjugated segment) along the conjugated π-electron system of the backbone. Moreover, in π-conjugated polymers on-chain chemical defects and/or torsional displacements can create conjugation barriers, thus leading to immobilization and spatial confinement of the formed excitons. As a consequence of these electronic properties, π-conjugated polymers are considered to be composed of a distribution of effectively conjugated segments (the so-called density of states DOS) and concomitantly a distribution of energies.[16−18] Therefore, the photophysics of conjugated polymers reflects the properties of an ensemble of chromophores of varying π-conjugation length with consequences in the emission spectra and excitation dynamics.[19−23]

Following light absorption, photophysical processes including radiative and nonradiative decay dissipate the absorbed energy. In addition, within the excited state lifetime of a CP, the electronic excitation (exciton) can migrate/delocalize toward lower energy sites/segments within the DOS (experimentally observed as spectral diffusion of the emission spectra occurring on a time scale of picoseconds to nanoseconds) until it becomes confined as a result of spatial isolation or a

Received: February 18, 2013
Revised: May 26, 2013

   dx.doi.org/10.1021/jp4017163 | J. Phys. Chem. B XXXX, XXX, XXX−XXX

conformational relaxation of the excited state.[17] Hereby, energy migration/transfer and conformational relaxation are competing processes. Energy migration is driven by through-bond interactions within the π-conjugated chain until the (accessible) lowest energy chromophores/segments are populated (where light emission can take place for radiative decay).[3,5] Conformational relaxation processes[24] also influence the time evolution of the emission spectrum of π-conjugated polymers. In contrast to the fast Franck−Condon relaxation, conformational relaxation (mainly due to friction of the side chains of the CPs in contact with solvent molecules during their displacement) generally occurs on a longer time scale ranging between 100 fs and 1 ns that is comparable to the time scale of the excitation energy migration/transfer.[16] Competition between conformational relaxation and excitation energy migration/transfer therefore determines the decay in isolated chains of π-conjugated polymers.[16,24,25]

The excited-state characteristic of CPs provides important information for a better understanding of the decay processes. A comprehensive characterization of the photophysical properties of π-conjugated polymers is therefore crucial for practical applications. The photophysical properties are strongly determined by chemical structure and molecular weight, by the solvent from which the polymer is processed (e.g., spin- or drop-cast), and by chain conformation and interchromophoric energy transfer.[26,27] However, even under well-defined conditions of sample preparation, neither energy migration/transfer nor chain conformation can be directly measured or controlled.[28] As a consequence of this, indirect ways have been used to probe the contributions of the two excited-state deactivation pathways. One of the approaches is the measurement of fluorescence lifetime transients of single polymer chains with low and high temporal resolution.[29−31] Another approach investigates the energy transfer processes in π-conjugated polymers by measuring the polarization anisotropy of single-chain fluorescence excitation and emission.[4,24,28]

An additional approach is made in the present contribution in which a series of poly[9,9-di(ethylhexyl)fluorene], PF2/6, fractions with different degrees of polymerization (DP) were investigated by steady-state and time-resolved fluorescence techniques as a function of temperature and solvent viscosity in order to clarify the nature of the decay processes (energy migration/transfer vs conformational relaxation). In particular, the influence of the chain length is discussed, thus giving, to the best of our knowledge, a comprehensive picture of the excited-state deactivation dynamics in CPs of different molecular weight.

EXPERIMENTAL SECTION

Synthesis. The synthesis of poly[9,9-bis(2-ethylhexyl)-fluorene], PF2/6, was accomplished in a standard homocoupling protocol after Yamamoto as described by Grell et al.[32] The different PF2/6 fractions were isolated by preparative scale size exclusion chromatography (GPC). The molecular weights M_n/M_w for the four PF2/6 fractions have been measured by GPC (polystyrene calibration) and were found to be 2600/4000, 5200/8100, 11600/33000, and 45000/160000 with DP of 5, 10, 39 and 205, respectively; see Table 1 for more details. It is worth noting that the M_w values of PF2/6 from GPC analyses with PS calibration are overestimated by 70−100% due to parallel SLS measurements [see ref 33].

Photophysical Measurements. All solvents used were of spectroscopic or equivalent grade. Absorption and fluorescence spectra were recorded on Shimadzu UV-2100 and Horiba-Jobin-Ivon SPEX Fluorog 3-22 spectrometers, respectively.

Table 1. Physical Characteristics of the Investigated PF2/6 Samples[a]

DP	$\bar{M}_n$ (g mol^{-1})	$\bar{M}_W$ (g mol^{-1})	PD
5	2600	4000	1.54
10	5200	8100	1.56
39	11600	33000	2.61
205	45000	160000	3.56

[a]Mean and weight average molecular weights ($\bar{M}_n/\bar{M}_w$), polydispersity (PD), and the degree of polymerization (DP) as calculated from $\bar{M}_w$.

The fluorescence spectra were corrected for the wavelength response of the system. For the steady-state and time-resolved emission experiments, the optical density of the solutions at the excitation wavelength was kept below 0.1 to avoid aggregation effects. Fluorescence quantum yields were measured using quinine sulfate (in 0.5 M H_2SO_4 solution, ϕ_F = 0.546[34]) as standard.

Fluorescence decays were measured using a home-built TCSPC system with a time resolution of ∼3 ps that has been described elsewhere.[35] Alternative measurements of the pulse profile at the excitation wavelength and the sample emission were performed until 5 × 10^3 counts at the maximum were reached. The fluorescence decays were analyzed using the modulating functions method of Striker with automatic correction for the photomultiplier "wavelength shift".[36] Temperature control was achieved using a home-built system based on cooled nitrogen and electric heating.

RESULTS AND DISCUSSION

In Table 1, mean number-average ($\bar{M}_n$) and weight-average molecular weights ($\bar{M}_w$) and polydispersity (PD = $\bar{M}_n/\bar{M}_w$) of the investigated PF2/6 polymers are presented. On the basis of the $\bar{M}_w$ data, the degrees of polymerization (DP) were calculated to be between 5 and 205 (Table 1).

Spectral Properties for the PF2/6 Polymers. Figure 1 presents the absorption and fluorescence emission spectra of the PF2/6 fractions in toluene at 293 K. At room temperature the solution absorption spectra display the characteristic unstructured absorption band of PF2/6;[37−40] see Figure 1 and Table 2. Contrary to the absorption spectra, the room

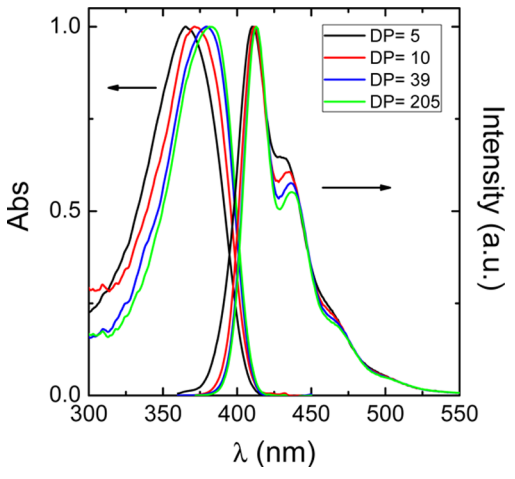

Figure 1. Normalized absorption and fluorescence emission spectra for the PF2/6 fractions (n = 5−205) in toluene at T = 293 K.

dx.doi.org/10.1021/jp4017163 | J. Phys. Chem. B XXXX, XXX, XXX−XXX

Table 2. Absorption (λ_{max}^{Abs}) and Emission (λ_{max}^{Fluo}) Wavelength Maxima, Stokes Shift (Δ_{SS}), and Fluorescence Quantum Yields (ϕ_F) Obtained in Toluene and Decalin (in Parentheses) for the PF2/6 Polymer Fractions[a]

DP	λ_{max}^{Abs} (nm) at 293 K	λ_{max}^{Fluo} (nm) at 293 K	Δ_{SS} (cm^{-1})	ϕ_F at 293 K
5	366 (365)	410, 430 (407, 428)	2932 (2827)	0.75 (0.79)
10	372 (372)	412, 434 (409, 430)	2610 (2432)	0.84 (0.83)
39	377 (377)	413, 436 (410, 433)	2312 (2135)	0.82 (0.83)
205	382 (380)	413, 438 (410, 434)	1965 (1926)	0.86 (0.82)

[a]The underlined values are the wavelength maxima; see text for more details.

temperature fluorescence emission spectra reveal a structured emission band, which is a characteristic feature of this and of related polymers, thus showing that with PF2/6 different main chain geometries are adopted in the ground and in the excited state.[37−40]

The observed spectral red shift in the absorption spectra upon going from n = 5 to n = 205 (~16 nm) shows that the π-delocalization degree (i.e., the effective conjugation length) increases with the size of the polymer chain, with the saturation still not fully finished for DP = 39. However, for the emission spectra a much smaller red shift (of ~3 nm) is observed upon going from n = 5 to n = 39, consistent with the emission originating from a relaxed state (obtained after conformational relaxation) rather than from a (instantaneously formed) Franck−Condon state.

For short chain PF2/6 (with DP = 5) a comparison with the literature shows that upon going from toluene (solvent orientation polarizability, Δf = 0.013) to the more polar solvent CH_2Cl_2 (Δf = 0.22) only a minor red shift in the absorption and emission maxima (λ_{max}^{Abs} = 366 nm vs 370 nm and λ_{max}^{Fluo} = 410 nm vs 416 nm respectively) is observed, thus giving once more support to the emission occurring from a relaxed excited-state.[41] The absorption and fluorescence emission spectra for the different PF2/6 fractions were also obtained in decalin solution at 293 K (see Figure S1 in Supporting Information). Spectroscopic features similar to those found in toluene solution (Table 2) were obtained.

Because of the low number of repeat units, the low $\bar{M}_W$ fraction (DP = 5) can be considered as an oligomer, that with DP = 10 as an intermediate, and those with DP of 39 and 205 as PF2/6 polymers with medium and high molecular weight.

From Figure 1 and Table 2 the fraction with DP = 5 shows the highest Stokes shift and a somewhat different shape of the emission spectrum (broadening of the high energy tail). This indicates a more localized excited state and therefore a more pronounced energetic difference between instantaneously formed and relaxed states. Indeed, as will be shown below, the energy barrier associated with the conversion between these two states is higher for the oligomer with DP = 5 if compared with the three other PF2/6 fractions.

In Figure 2 the temperature dependence of the fluorescence emission spectra is given for the PF2/6 fractions with DP of 10 and 205. When the temperature is decreased from 50 to −30 °C, for both samples a small red shift, accompanied by a better resolved vibronic structure of the spectra, occurs.

Dependence of ϕ_F with DP. Fluorescence quantum yields (ϕ_F) were measured in toluene and decalin solutions (Table 2). Within the experimental error similar ϕ_F values were found in the investigated solvents, in agreement with what was previously observed for the spectroscopic properties. The ϕ_F values found for the PF2/6 fractions (0.75−0.86) can be considered to be chain length independent, within the experimental error. A similar behavior was found for

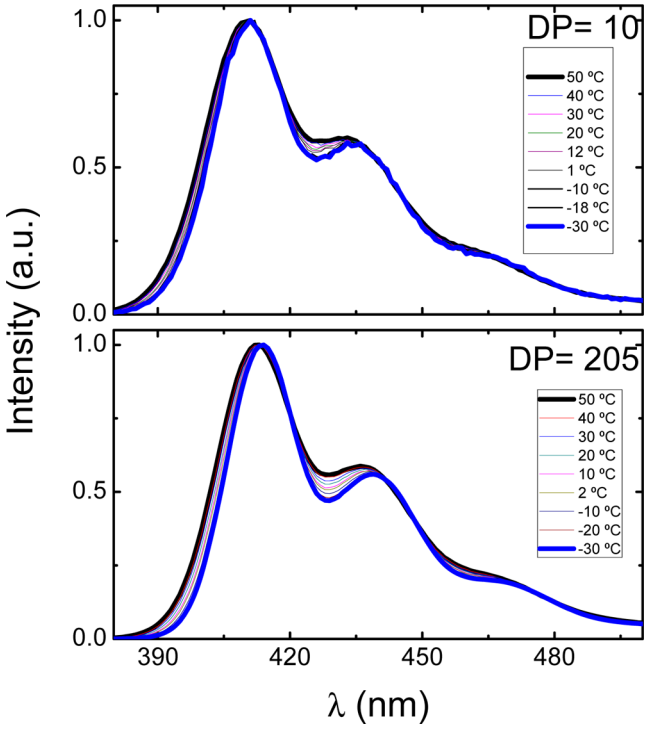

Figure 2. Normalized fluorescence emission spectra for PF2/6 fractions with DP = 10 and DP = 205 in toluene solution obtained as a function of temperature.

diphenylamino end-capped oligo(9,9-diarylfluorene)s (n = 2−5) where the ϕ_F values are more or less unaltered for n = 3−5 (ϕ_F of 0.86−0.93).[42] Moreover, in a series of 9,9-bis-(methylbutyl)-substituted oligofluorenes (n = 2−16) the long wavelength absorption maxima in chloroform solution was found to range from 330 to 382 nm (for comparison λ_{max} = 387 nm for the corresponding polymer) with a saturation starting at n = 6−7. The corresponding emission maxima vary from 363 to 412 nm (λ_{max} = 416 nm for the polymer). Typically, the convergence of the emission properties sets in for shorter oligomer lengths, pointing to a reduced dimension of the effectively conjugated segments in the excited state. The reported solid-state ϕ_F values for thin films decrease with n, from 0.75 (for n = 4) to 0.51 (n = 11); ϕ_F = 0.24 for the polymer.[43] For 9,9-di-*n*-hexylfluorene oligomers with n = 3−10 in THF solution the long wavelength absorption maxima are found between 348 and 384 nm (388 nm for the polymer) and the emission maxima are between 413 and 445 nm (445 nm for the polymer).[44]

Our measured ϕ_F values correspond well to values for the fluorene monomer (ϕ_F = 0.71 in methylcyclohexane),[34] a fluorene trimer 9,9,9′,9′,9″,9″-hexakis(octyl)-2,7′;2′,7″-trifluorene (ϕ_F = 0.78 in toluene), and various polyfluorenes (ϕ_F = 0.93 for PF2/6 in $CHCl_3$[45] or ϕ_F = 0.74−0.78, depending of

dx.doi.org/10.1021/jp4017163 | J. Phys. Chem. B XXXX, XXX, XXX−XXX

the solvent, for a PF2/6 sample with M_w = 210 000;[30] ϕ_F = 0.64−0.69 for 9,9-di-*n*-alkyl-substituted polyfluorenes with DP = 42−62 in THF[40]). On the basis of our data (Table 2), the ϕ_F value also remains unchanged with increasing DP (with a slightly smaller value for DP = 5). By comparison of our and literature data,[41] it is obvious that the alkyl substitution (linear, branched) clearly influences the chain conformation and consequently the degree of π-electron delocalization adopted by the oligo and polyfluorenes. However, within a series of identically substituted oligo/polyfluorenes, the convergence of the absorption properties starts with n = 6−7.[41]

Time Resolved Fluorescence. Fluorescence decays for the PF2/6 polymers were collected in solvents of different viscosity (toluene and decalin) as a function of the emission wavelength and temperature (see Supporting Information for complete data on the obtained fluorescence decay times and pre-exponential factors).

The fluorescence decays were found to be fitted with a sum of two exponentials, and in general the decay times do not show any significant variation when collected along the fluorescence spectra and are therefore independent of the emission wavelength. However, the same is not valid for the pre-exponential factors, found to vary with the emission wavelength. This calls for a global (simultaneous) analysis of the decays.

The analysis of the PF2/6 decays in toluene reveals the presence of fast (34−41 ps) and longer decay (387−452 ps) components (Tables 3 and 4) in agreement with the work of

Table 3. Fluorescence Decays Times (τ_i) and Pre-Exponential Factors (a_{ij}) for the PF2/6 Polymers in Toluene Solution at T = 293 K Obtained with λ_{exc} = 392 nm[a]

DP	λ_{em} (nm)	τ_2 (ps)	τ_1 (ps)	a_{i2}	a_{i1}	χ^2
5	400	41	452	0.411	0.589	1.15
	420			−0.127	1.000	1.01
	520			−0.195	1.000	1.09
10	400	41	423	0.438	0.562	1.34
	420			−0.156	1.000	1.04
	520			−0.193	1.000	1.13
39	400	36	392	0.447	0.553	1.35
	420			−0.133	1.000	1.05
	520			−0.173	1.000	1.22
205	400	30	387	0.462	0.538	1.29
	420			−0.141	1.000	1.06
	520			−0.143	1.000	1.10

[a]For a better judgment of the quality of the fits, also presented are the χ^2 values. The χ^2 values for a good adjustment should vary between 1.0 and 1.35. The data presented were obtained by global (simultaneous analysis of the decays at the three emission wavelengths) analysis of the decays.

Dias et al.[37] (PF2/6 with M_w = 250 000 and DP = 321). As listed in Table 3 (and again in agreement with literature data[37]), the pre-exponential factors are positive when the decays are collected at the onset (blue edge of the spectra) of the emission band (λ_{em} = 400 nm). When the emission decays are collected at $\lambda_{em} \geq$ 420 nm (low energy side of the emission band), a negative amplitude (rise time) associated with the shortest decay time is observed.

Dependence with Solvent Viscosity. The gradual increase in the negative pre-exponential factor (associated to the fast decay time component) with the increase in the

Table 4. Fluorescence Decays Times (τ_i) and Pre-Exponential Factors (a_{ij}) for PF2/6 Polymers in Decalin Solution at 293 K oObtained with λ_{exc} = 282 nm and χ^2 for a Better Judgment of the Quality of the Fits[a]

DP	λ_{em} (nm)	τ_2 (ps)	τ_1 (ps)	a_{i2}	a_{i1}	χ^2
5	400	100	460	0.397	0.603	1.18
	420			−0.076	1	1.03
	520			−0.198	1	1.1
10	400	84	453	0.402	0.598	1.21
	420			−0.124	1	1.05
	520			−0.138	1	1.04
39	400	73	414	0.447	0.553	1.27
	420			−0.143	1	1.07
	520			−0.148	1	1.06
205	400	60	390	0.444	0.556	1.29
	420			−0.187	1	1.04
	520			−0.161	1	1.11

[a]The data presented were obtained by global (simultaneous analysis of the decays at the three emission wavelengths) analysis of the decays.

emission wavelength, and the dominance of the longer decay time in the low energy part of the emission spectra, has been shown for PF2/6[37,38] (and in other related CPs[35,46−48]) to indicate that the relaxed structure of the polymer (longer decay time) is being formed (in the excited state) at the expense of the nonrelaxed structure (shorter decay time).[24,48,49] The longer component is clearly coupled to the relaxed structure of the excited chromophoric segment as indicated by the monoexponential decay values observed for oligofluorenes with n = 5−6, $\tau_F \approx$ 0.6 ns, although an additional short component associated with a rise time was also reported in this study.[41]

However, the shorter component is, as will be shown and discussed below, associated not only with the conformational relaxation process but also with the solvation dynamics contribution.

On going from toluene to the more viscous solvent decalin the τ_1 values, and associated pre-exponential factor, remain effectively unchanged within the experimental error (Tables 3 and 4). However, this is not valid for the shorter decay time (τ_2), where a significant increase in the decay time value is observed going from toluene to decalin: 30−41 ps in toluene vs 60−100 ps in decalin.

Noteworthy (Tables 3 and 4), the shorter decay time decreases with increasing DP from 41 to 30 ps in toluene solution and, more pronounced, in decalin, from 100 to 60 ps. The differences between toluene and decalin solution clearly indicate that a conformational relaxation process is going on that is dependent on the polymer chain length. Although this is not unexpected, it illustrates the influence of the chain length on the conformational relaxation process in PF2/6.

Since the inherent solvent barrier should be unchanged for all PF2/6's, the chain length seems to be a critical factor influencing the decay mechanism.

Dependence with Temperature. Additional information regarding the excited state decay pathways of the different PF2/6 fractions comes from the temperature dependence of the fluorescence decay (Figure 3 and Tables S1−S8 in Supporting Information). For all the PF2/6 fractions the long-lived component (τ_1) is found (within the temperature range investigated, −20 to +50 °C) to be temperature independent. However, a clear temperature dependence is observed for the

dx.doi.org/10.1021/jp4017163 | J. Phys. Chem. B XXXX, XXX, XXX−XXX

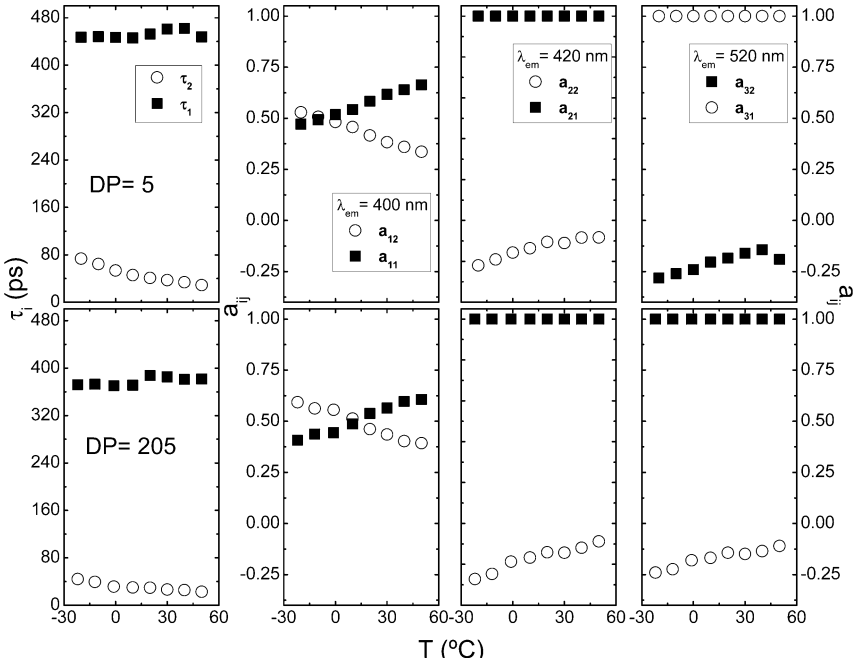

Figure 3. Temperature dependence of the fluorescence decay times (τ_i) and pre-exponential factors (a_{ij}) collected at λ_{em} = 400, 420, and 520 nm for PF2/6 with DP = 5 (top panels) and DP = 205 (bottom panels) in toluene solution (λ_{exc}= 392 nm). Data were obtained by global analysis of the decays.

fast component (τ_2), and the pre-exponential factors collected at 400 nm show an increasing contribution of this component at low temperature (Figure 3).

Kinetics of the Conformational Relaxation Process. The double exponential nature of the decays leads in a first approach to a kinetic formalism associated with the conformational relaxation process involving the instantaneous formation of A* (initial nonrelaxed structure), which can decay to the ground state or give rise to a second species B* (conformationally relaxed, more planar structure) also decaying to the ground state (Scheme 1).[37]

Scheme 1

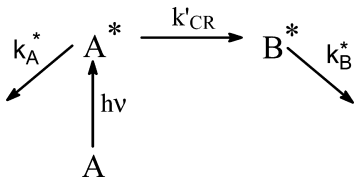

This can be considered to be a two-state system, assuming that no reversibility (B* → A*) exists,[37] and allows an estimation of a rate constant k'_{CR} (see Scheme 1) according to eq 1:[37]

$$k'_{CR} = \frac{1}{\tau_2} - k_A^* \tag{1}$$

where k_A^* is the reciprocal of τ_A, the decay time in the absence of competitive processes (conformational relaxation, CR, and energy transfer, ET) that can be obtained from a model compound where these processes are absent. A proper model system for our calculation is the ladder-type poly(*p*-phenylene), MeLPPP, a rigid π-conjugated polymer in which conformational changes are per se precluded.[38] Note that both PF2/6 and MeLPPP are composed of very similar poly(*p*-phenylene) backbones, only with a different alkyl substitution pattern.

However, the simultaneous presence of nonrelaxed (A) and relaxed (B) structures at room temperature cannot be excluded. This leads to a new kinetic scheme where two species (A and B) are already present in the ground state. This is further illustrated in Scheme 2. Moreover, in this scheme the reversibility between the two species in the excited state (k_{-CR}) is also equated.

Scheme 2

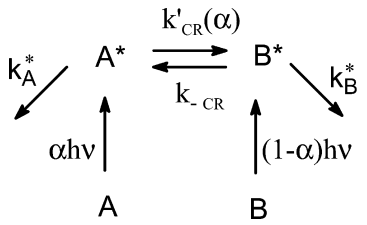

According to Scheme 2 the excited state concentration time dependence of the species A* and B* is given by the following (see Supporting Information for further details):[50,51]

$$[A^*] = a_{11}e^{-\lambda_1 t} + a_{12}e^{-\lambda_2 t} \tag{2}$$

$$[B^*] = a_{21}e^{-\lambda_1 t} + a_{22}e^{-\lambda_2 t} \tag{3}$$

where the λ_i are the reciprocal decay times of the shorter ($\lambda_2 = 1/\tau_2$) and of the longer ($\lambda_1 = 1/\tau_1$) species and a_{ij} are the pre-exponential factors. As previously demonstrated,[50,51] based on the decay parameters (a_{ij} and τ_i) and k_A^* (which is the reciprocal of the lifetime of the model compound, MeLPPP), it is possible to obtain all the unknowns in Scheme 2 (k_B^*, k'_{CR}, k_{-CR}, and α), see Supporting Information.

The obtained conformational relaxation rates at 293 K in toluene and decalin solution are given in Table 5. These were

dx.doi.org/10.1021/jp4017163 | J. Phys. Chem. B XXXX, XXX, XXX−XXX

Table 5. Rate Constants for the Conformational Relaxation Process (k'_{CR} and $k'_{CR}(\alpha)$), Reversibility (B* → A*, k_{-CR}), and Deactivation (of the Relaxed B* Species, k_B^*) and Respective Activation Energy Values (E_a^{CR}), Considering Scheme 1,[a] Scheme 2,[b] or the Value Associated with the Shorter Decay Time[c] Obtained from Dynamic Stokes Shift Correlation Function (Eq 5), k_{CR}, in Toluene and Decalin for the PF2/6 Polymer Fractions at 293 K, and the Fraction (α) of Nonrelaxed (A) species in the Ground State

DP	$k'_{CR} \times 10^{10}$ $(s^{-1})^a$	$k'_{CR}(\alpha) \times 10^{10}$ $(s^{-1})^b$	α	E_a^{CR} (kJ mol^{-1})^a	E_a^{CR} (kJ mol^{-1})^b	$k_{-CR} \times 10^{10}$ $(s^{-1})^b$	$k_B^* \times 10^{10}$ $(s^{-1})^b$	$k_{CR} \times 10^{10}$ $(s^{-1})^c$	E_a^{CR} (kJ mol^{-1})^c
					Solvent = Toluene				
5	2.1	1.6	0.61	10.6	12.8	0.51	0.19	2.4	8.9
10	2.1	1.7	0.64	8.5	11.1	0.46	0.22	2.4	7.2
39	2.5	2.0	0.67	6.7	9.2	0.46	0.24	2.8	5.8
205	3.0	2.6	0.73	6.4	8.7	0.45	0.25	3.3	5.7
					Solvent = Decaline				
5	0.69	0.51	0.57	21.4	23.4	0.22	0.18	1.0	10.7
10	0.88	0.71	0.69	10.2	10.0	0.19	0.20	1.2	6.5
39	1.1	0.88	0.70	13.7	14.5	0.19	0.23	1.4	9.2
205	1.4	1.1	0.69	9.1	8.7	0.25	0.24	1.7	7.1

[a]In the case of Scheme 1, k'_{CR} is obtained with eq 1. [b]In the case of Scheme 2, k_{CR}, k_{-CR}, and α are obtained with eq S28, S29, and S30 (Supporting Information); k_B^* is obtained from eq S27 (Supporting Information). [c]The k_{CR} value is obtained from the reciprocal of the τ_2 decay time; see text for further discussion.

obtained considering Scheme 1 (k'_{CR}) and Scheme 2 [$k'_{CR}(\alpha)$], i.e., with excitation of only the nonrelaxed species (A in Scheme 1) or simultaneous excitation of nonrelaxed (A in Scheme 2) and relaxed (B in Scheme 2) species together with the lifetime of the model compound MeLPPP ($k_A^* = 1/\tau_A$) at T = 293 K with a value of 319 ps (see Table S9 in Supporting Information). Moreover, from Scheme 2 and eq S30 (in Supporting Information) it is also possible to obtain the fraction of species A (α) and B ($1 - \alpha$) in the ground state, which is also presented in Table 5. The dependence of k_{-CR} and k_B^* with the polymers' PD is also given in Table 5.

Also relevant is that the contribution of the (A) nonrelaxed (α in Table 5) vs the (B) relaxed ($1 - \alpha$) species is 64−74% for A and 36−26% for species B and that this ratio (A/B) gradually increases with the size of the polymer. This means that the larger the PF2/6 polymer, the greater is the contribution of the nonrelaxed species.

Moreover, the fact that the sum of the pre-exponential factors ($a_{21} + a_{22}$) do not cancel out at longer emission wavelengths [in Tables 3 and 4 and Tables S1−S8 (in Supporting Information)] is a direct consequence of eqs S11, S14, and S15 (in Supporting Information), that is, at the excitation wavelength both A and B species absorb.

Data in Table 5 show that, considering the simplified kinetic Scheme 1, the values for k'_{CR} vary for the different PF2/6 polymer fractions between (2.1−3.0) × 10^{10} s^{-1} in toluene and (0.69−1.4) × 10^{10} s^{-1} in decalin, whereas when the simultaneous presence in the ground state of relaxed and nonrelaxed species is considered (Scheme 2), the obtained rate constants are now decreased varying from 1.6 × 10^{10} to 2.6 × 10^{10} s^{-1} in toluene and from 0.51 × 10^{10} to 1.1 × 10^{10} s^{-1} in decalin. The values for the k_{CR} ($\equiv 1/\tau_2$) will be discussed below.

By use of the Stokes−Einstein (SE) relation ($k \approx \eta^{-\gamma}$), the dependence of the above relaxation rate constant with solvent viscosity can be presented in a log−log plot (ln k'_{CR} vs ln η) with γ = 1 if the SE equation holds, that is, if the process is a pure diffusion-controlled process. The log−log plot of $k'_{CR}(\alpha)$ and k'_{CR} vs the viscosity (at different temperatures) is plotted in Figure 4. However, the obtained γ values are, for DP 5, 1.44 and 1.18 for $k'_{CR}(\alpha)$ and k'_{CR}, respectively, which are physically unrealistic.

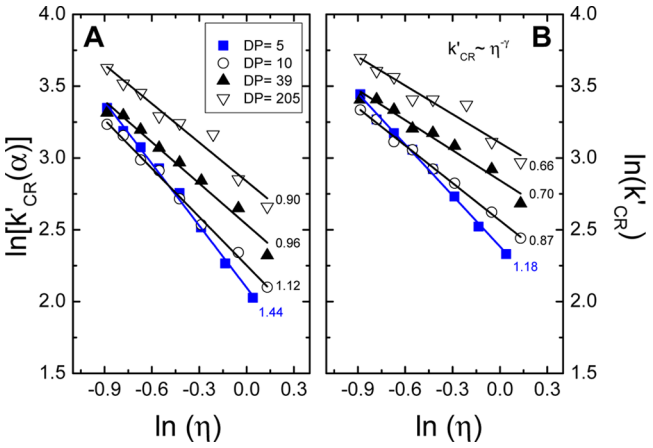

Figure 4. Log−log plot of $k'_{CR}(\alpha)$ and k'_{CR} vs viscosity (toluene) at different temperatures. Viscosity values were taken from ref 52. After each set of data the γ value, obtained from the linear fit, is presented.

This shows that the fast dynamic component (observed as a decay at lower wavelengths (the band onset) and as a rise at longer wavelengths (band tail)) must be interpreted as a time dependent red shift of the emission spectra that results from solvent and conformational relaxation.[46] For this to be equated the time-resolved spectra of these compounds ought to be obtained. Therefore, the emission spectra of the PF2/6 with DP5 were obtained at different times after excitation, $S(\lambda,t)$, and were constructed with the fluorescence decays $I(t,\lambda)$ in toluene (with the decay times 41 and 452 ps and the preexponential factors collected between 390 and 495 nm) after normalization of the integrated decay to the steady-state fluorescence intensity at the respective emission wavelength $S(\lambda,\infty)$ (see eq 4).[46,53]

$$S(\lambda,t) = (t,\lambda)\frac{S(\lambda,\infty)}{\int_0^\infty I(t,\lambda)\,dt} \tag{4}$$

In the case of PF2/6 with DP5 the spectra red-shifts 3 nm from 0 to 100 ps, after which the spectra become identical to the steady-state spectra (see Figure 5). This time-dependent red shift of the spectrum should therefore be analyzed with the

dx.doi.org/10.1021/jp4017163 | J. Phys. Chem. B XXXX, XXX, XXX−XXX

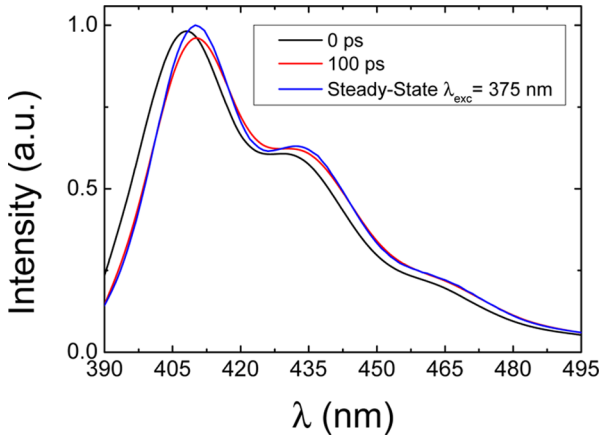

Figure 5. Normalized time-resolved emission spectra for PF2/6 DP = 5 in toluene obtained at 0 and 100 ps and compared with the steady-state spectra at T = 298 K. The spectral reconstruction was obtained with eq 4 and with decays recorded with an interval of 5 nm.

Stokes shift correlation function (the "dynamic Stokes shift") $C(t)$ (see eq 5).[46,53]

$$C(t) = \frac{\nu(t) - \nu(\infty)}{\nu(0) - \nu(\infty)} \quad (5)$$

where $\nu(t)$, $\nu(0)$, and $\nu(\infty)$ stand for the frequency of the emission maximum at time t, t = 0, and t = ∞ (steady state), respectively. The frequency corresponding to the maximum of the steady state spectra (λ = 410 nm) was further used to generate the correlation function in Figure 6.

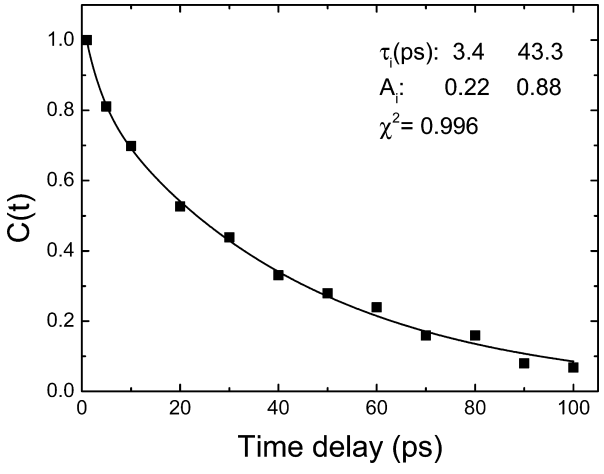

Figure 6. Stokes shift correlation function (SSCF) for PF2/6, DP = 5 in toluene at T = 293 K. Shown as inset are the decay times and associated pre-exponential factors together with the χ^2 value.

The obtained $C(t)$ correlation function is correctly fitted with a biexponential law with decay times of 3.4 ps (22%) and 43.3 ps (88%). The shorter component has a value that can be considered to be within the range of values found for the mean relaxation time of a number of dipolar and nondipolar solute–solvent pairs and should be associated with the slow part of the solvation dynamics.[46,54] Extensive studies have been performed with coumarin C153 in a broad range of solvents with a reported solvation time of 2.7 ps in toluene (a solvation mechanism where the solute–solvent coupling is made through electrostatic interactions, mainly dipole–quadrupole interactions).[54,55] In the case of a *p*-phenylene vinylene (PPV) trimer, a value of 5.5 ps was found in methylcyclohexane.[46] However, the longer decay time (43.3 ps) obtained from the Stokes shift correlation function in Figure 6 is too long to be associated with the dynamics of solvation and, similar to that reported with the PPV trimer,[46] should be assigned to the conformational relaxation process of the PF2/6 with DP = 5. As mentioned, this conformational process occurring with the PF2/6 (DP5) oligomer results from twisted ground-state-like conformations to more planar conformations in the excited state, compatible with the broad nature of the absorption band in contrast with the resolved nature of the emission band in Figure 1, a behavior observed with other organic conjugated oligomers and polymers.[35,37,38,45,46,56−58] This conformational process involves the contribution of the lateral (ethyl–hexyl) chains by storing and dissipating the stresses induced by photoexcitation.[59]

Moreover, this longer component obtained from the Stokes shift correlation function (in Figure 6) is clearly associated with the value in Table 3 (41 ps) for the relaxed (or more planar conformations) excited state. Hence, the direct analysis of the (double-exponential) decays provides, within the experimental error (41 ps vs 43.3 ps), the same value for the relaxation decay time. Therefore, both the $C(t)$ (eq 5) and exponential analysis (eqs 2 and 3) provide the same result for this relaxation time. As a result, the reciprocal of the decay time τ_2 should be, indeed, regarded as the rate constant associated with the conformational relaxation process, k_{CR}.

The k_{CR} values ($\equiv 1/\tau_2$) are shown in Table 5 and, in this case, were found to be in the range (2.4−3.3) × 10^{10} s^{-1} in toluene and (1.0−1.7) × 10^{10} s^{-1} in decalin. These values are all in good agreement with the values reported for PF2/6 with DP = 321 (2.5 × 10^{10} and 1.5 × 10^{10} s^{-1}, respectively).[37] As expected, on going from toluene to the more viscous solvent decalin, a decrease in the k_{CR} value is obtained. Noteworthy is the increase in k_{CR} values with the increase in the polymer size for the two solvents investigated (see Table 5).

Furthermore, from the temperature dependence of the fluorescence decays of the MeLPPP polymer (where conformational relaxation is absent) it was seen that within experimental error the τ_A value is approximately constant with temperature (with values ranging from 310 to 319 ps; see Table S9 in Supporting Information). This allows obtaining the rate constants k'_{CR} and $k'_{CR}(\alpha)$ as a function of temperature and therefore the associated activation energies (Table 5).

However, according to the discussion above to obtain the activation energy of the conformational relaxation process (E_a^{CR}) for the different PF2/6 fractions, it is more adequate to use k_{CR} ($\equiv 1/\tau_2$). Indeed, by plotting of $\ln(k_{CR} \equiv 1/\tau_2)$ vs $1/T$ (Arrhenius-type plot, Figure 7), the E_a^{CR} values are obtained from the observed slopes and were found to be in the range 5.7−8.9 kJ mol^{-1} in toluene and 6.5−10.7 kJ mol^{-1} in decalin solution (see Table 5). Again, these values are in very good agreement with literature results for PF2/6 with DP = 351, E_a^{CR} ≈ 9.7 and 9.9 kJ mol^{-1} in decalin and methylcyclohexane solution, respectively.[37]

From Table 5 it is also worth mentioning that the activation energies when considering Scheme 2 (simultaneous presence in the ground state of nonrelaxed, A, and relaxed, B, species) are always higher that those obtained considering only the excitation of the A species (Scheme 1). Nevertheless, in general the activation energies for the conformational relaxation process in our PF2/6 fractions are lower than the activation

dx.doi.org/10.1021/jp4017163 | J. Phys. Chem. B XXXX, XXX, XXX−XXX

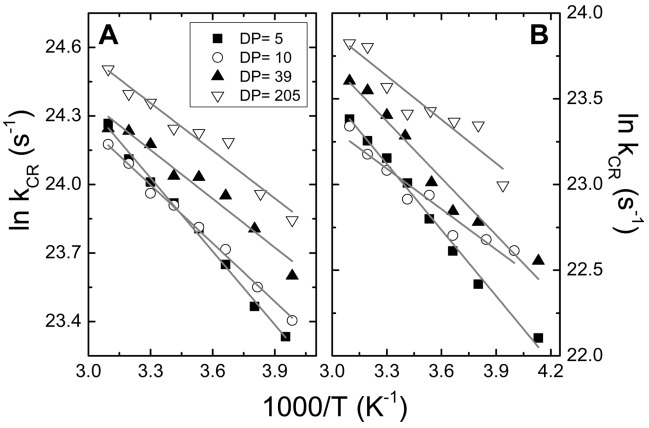

Figure 7. Arrhenius-type plots for relaxation rate constant ($k_{CR} \equiv 1/\tau_2$) for PF2/6 polymers in (A) toluene and (B) decalin solution.

energies $E(T/\eta)$ for pure viscous flow of the solvent (12.9 kJ mol^{-1} for toluene).[60]

Once more, from the log–log plot [$\ln(k_{CR} \equiv 1/\tau_2)$ vs $\ln \eta$], with the exception of the oligomer fraction with DP = 5 (where $\gamma \cong 1$), the obtained γ values are lower than unity (see Figure 8), showing that the solvent frictional forces counteracting the

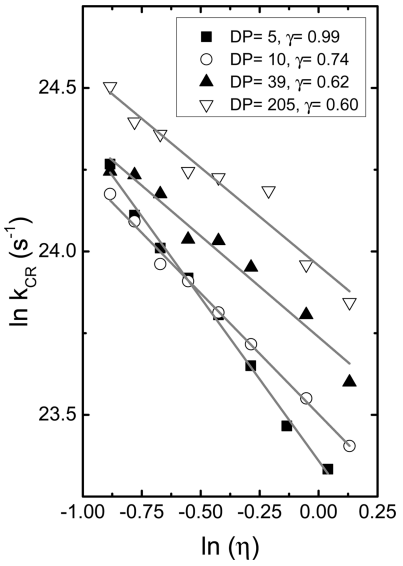

Figure 8. Log–log plot of k_{CR} ($\equiv 1/\tau_2$) vs viscosity (toluene) at different temperatures. Viscosity values were taken from ref 52.

conformational relaxation of the oligo/polyfluorene chains are less effective than those that may be predicted from the macroscopic solvent friction ($k \approx \eta^{-1}$).[46] This is in agreement with the observation that the E_a^{CR} values found for the investigated PF2/6 fractions are lower than the activation energies $E(T/\eta)$ for viscous flow of the solvent. Moreover, it is also worth noting that the PF2/6 oligomer (DP = 5) has a different behavior from what is found for the PPV trimers,[46,59,61] where γ is always found to be <1. In fact, in the case of the PPV trimers with different lateral chains, smaller γ values were observed with longer lateral chains leading to the conclusion that the side chains controlled the overall relaxation process.[46] Indeed, $\gamma < 1$ was associated with the fact that the relatively small amplitudes of the side chain displacement during the (conformational) relaxation process suffer a lower solvent friction.[46] Also, with the PPV trimers the increase in size of the side chains was argued to reduce the cohesion of the solute solvent pair, increasing what was considered the "nanoviscosity" of the trimer.[59]

In the present study, since the oligomer (DP = 5) follows a pure diffusion controlled process, it appears that the lateral side chains are not determinant to the relaxation process but that it is the polyfluorene backbone that controls the overall relaxation process. As a matter of fact, with the investigated PF2/6 polymers (DP ≥ 10) k_{CR} is now proportional to $\eta^{-\gamma}$ instead of the normal Stokes–Einstein proportionality behavior (η^{-1}) with γ depending on the number of PF2/6 units; see the slope (γ) values in Figure 8.

Also, within experimental error and in agreement with the k_{CR} values (Table 5), the activation barrier for the conformational relaxation process is dependent on the polymer chain length: it decreases with increasing chain length. As previously mentioned, the increased Stokes shift found for the oligomer fraction with DP = 5 (see Table 2) shows that the structural/geometrical differences between the ground and the excited state should be more pronounced in relation to the higher molecular weight fractions. For the oligomeric fraction (DP = 5), the activation energy for conformational relaxation is higher, and since the γ value is near unity, it is expected that the segmental movements from the nonrelaxed into the relaxed (more planar) excited state are purely solvent-diffusion-controlled. For the higher molecular weight PF2/6 fractions the activation energy barrier for conformational relaxation is lower, which means that smaller forces for torsional displacements are needed. This can be explained in terms of the chain structure of the polymer. Indeed, with poly(9,9-dioctylfluorene-2,7-diyl), PF8, it was seen that in dilute toluene solutions this polymer is present as fully dissolved polymer coils.[62] In our case it is expected that similar coiled chain structures are adopted by the higher molecular weight PF2/6 fractions and consequently a decreased solvent friction should occur thus, leading to the observed decrease from $\gamma = 1$ to $\gamma = 0.6$.

For oligofluorenes the relaxation is considered to be purely conformational in time scales between 10 and 300 ps, becoming faster with decreasing chain length and solvent viscosity or increasing temperature. However, for PF2/6 (with a DP of ~60) in toluene, *n*-octane, and decalin solvent solutions, it was suggested that both conformational relaxation and exciton migration are present.[38] In contrast, others[30] reported that a single exponential with a lifetime of 357–381 ps (depending on solvent) is sufficient to describe the fluorescence decays of a 9,9′-dioctylfluorene end-capped with *N*-(2-benzothiazole)-1,8-naphthalimide (M_w = 210 000, DP = 538). Nonetheless, the authors mention that besides the major long-lived component a fast component of about 40 ps was also observed, but this minor short living component was neglected because it was considered to contribute with less than 3%.[30]

In the present work, within our time resolution (~3 ps), the data obtained for the PF2/6 fractions confirm that conformational relaxation is the dominant excitation energy deactivation process, although occurrence of excitation energy migration at shorter time scales cannot be discarded.

CONCLUSION

Four PF2/6 fractions of increasing molecular weight (ranging from DP of 5 to 205) were investigated in dilute solution. The fluorescence decays of these isolated chains were found to be biexponentials with rising and decay components. From the

dx.doi.org/10.1021/jp4017163 | J. Phys. Chem. B XXXX, XXX, XXX–XXX

observed temperature and solvent viscosity dependence, the fast component was assigned to a (fast) conformational relaxation process that occurs within the excited-state lifetime of the polymers. In agreement with the double-exponential nature of the decays, a model involving two species (nonplanar and more planar conformers, A and B species, respectively) and excitation of a single (A) species and of the two (A and B) species was applied. However, it was found that the log−log plot of the relaxation rate constants [k'_{CR} and $k'_{CR}(\alpha)$] (obtained with these two kinetic schemes) vs the solvent viscosity dependence with temperature in toluene led to unrealistic γ values for the dependence with viscosity ($\eta^{-\gamma}$, with $\gamma = 1$ for the Stokes−Einstein rate diffusion law). The Stokes shift correlation function was then used for the PF2/6 with DP = 5. Two components were obtained: a shorter one with 3.4 ps (associated with the relaxation time associated with the slow part of the solvation dynamics process) and a longer one with 43.3 ps associated with the conformational/torsional relaxation process, which is identical to the shorter component found in the biexponential decays (τ_2). The reciprocal of this (τ_2) value was therefore considered as the value for the k_{CR} and used to obtain the temperature and viscosity dependent plots for the remaining PF2/6 polymers. It was found that the rate constant for this process increases with DP and that the energy barrier, associated with the conformational relaxation process, was found to significantly depend on the PF2/6 chain length, decreasing with increasing chain length and thus showing that for the PF2/6 oligomer fraction the structural differences between the nonrelaxed and relaxed excited state are more pronounced when compared to the higher molecular weight PF2/6 fractions. The study showed that the size of the PF2/6 skeleton influences the dynamics and photophysics of the polymers. Finally it is important to emphasize that by making this approach, i.e., using kinetic formalisms that imply (i) the investigation of the system with a two-state model (double-exponential decay analysis of the fluorescence decays) followed by (ii) taking into account a time-dependent red shift of the emission spectrum (using the Stokes shift correlation function) in order to clearly equate the contribution of the solvation dynamics process, we believe we have designed a correct strategy of analysis of these systems where the conformational/torsional relaxation process dominates the deactivation of the excited state.

■ ASSOCIATED CONTENT

Supporting Information

Complete equations leading to the solution of Scheme 2, together with (i) the absorption and fluorescence emission spectra for the PF2/6 fractions (n = 5−205) in decalin at T = 293 K (Figure S1), (ii) the dependence of the rate constants for conformational relaxation k'_{CR} and k'_{CR} (α), with DP in toluene and decalin (Figure S2), (iii) the fluorescence decays times and pre-exponential factors obtained at different temperatures for the PF2/6 polymers with DP = 5−205 in toluene and decalin (Tables S1−S8), and (iv) the fluorescence decay times for the MeLPPP polymer in toluene solution collected as a function of temperature (Table S9). This material is available free of charge via the Internet at http://pubs.acs.org.

■ AUTHOR INFORMATION

Corresponding Author

*E-mail: sseixas@ci.uc.pt.

Notes

The authors declare no competing financial interest.

■ ACKNOWLEDGMENTS

The Portuguese Science Foundation (FCT) FCT and FEDER/COMPETE are acknowledged for financial support (Program C2008-DRH05-11-842).

■ REFERENCES

(1) Schindler, F.; Jacob, J.; Grimsdale, A. C.; Scherf, U.; Müllen, K.; Lupton, J. M.; Feldmann, J. Counting Chromophores in Conjugated Polymers. *Angew. Chem., Int. Ed.* **2005**, *44* (10), 1520−1525.

(2) Pina, J.; Burrows, H. D.; Seixas de Melo, J. S. Excited State Dynamics in π-Conjugated Polymers. In *Specialist Periodic Reports in Photochemistry*; Albini, A., Ed.; RSC: Cambridge, U.K., 2011; Vol. *39*, pp 30−64.

(3) Van Averbeke, B.; Beljonne, D. Conformational Effects on Excitation Transport along Conjugated Polymer Chains. *J. Phys. Chem. A* **2009**, *113* (12), 2677−2682.

(4) Collini, E.; Scholes, G. D. Electronic and Vibrational Coherences in Resonance Energy Transfer along MEH-PPV Chains at Room Temperature. *J. Phys. Chem. A* **2009**, *113* (16), 4223−4241.

(5) Van Averbeke, B.; Beljonne, D.; Hennebicq, E. Energy Transport along Conjugated Polymer Chains: Through-Space or Through-Bond? *Adv. Funct. Mater.* **2008**, *18* (3), 492−498.

(6) Scheblykin, I. G.; Yartsev, A.; Pullerits, T.; Gulbinas, V.; Sundstrom, V. Excited State and Charge Photogeneration Dynamics in Conjugated Polymers. *J. Phys. Chem. B* **2007**, *111* (23), 6303−6321.

(7) Pauck, T.; Hennig, R.; Perner, M.; Lemmer, U.; Siegner, U.; Mahrt, R. F.; Scherf, U.; Müllen, K.; Bässler, H.; Göbel, E. O. Femtosecond Dynamics of Stimulated-Emission and Photoinduced Absorption in a Ppp-Type Ladder Polymer. *Chem. Phys. Lett.* **1995**, *244* (1−2), 171−176.

(8) Cheng, Y. J.; Yang, S. H.; Hsu, C. S. Synthesis of Conjugated Polymers for Organic Solar Cell Applications. *Chem. Rev.* **2009**, *109* (11), 5868−5923.

(9) Martelo, L.; Jimenez, A.; Valente, A. J. M.; Burrows, H. D.; Marques, A. T.; Forster, M.; Scherf, U.; Peltzer, M.; Fonseca, S. M. Incorporation of Polyfluorenes into Poly(lactic acid) Films for Sensor and Optoelectronics Applications. *Polym. Int.* **2012**, *61* (6), 1023−1030.

(10) Albrecht, S.; Schafer, S.; Lange, I.; Yilmaz, S.; Dumsch, I.; Allard, S.; Scherf, U.; Hertwig, A.; Neher, D. Light Management in PCPDTBT:PC70BM Solar Cells: A Comparison of Standard and Inverted Device Structures. *Org. Electron.* **2012**, *13* (4), 615−622.

(11) Scherf, U.; Tian, H. Organic Electronics/Optics: For an Energetic Life. *Adv. Mater.* **2012**, *24* (5), 576−579.

(12) Friend, R. H. Conjugated Polymers. New Materials for Optoelectronic Devices. *Pure Appl. Chem.* **2001**, *73* (3), 425−430.

(13) Kallinger, C.; Hilmer, M.; Haugeneder, A.; Perner, M.; Spirkl, W.; Lemmer, U.; Feldmann, J.; Scherf, U.; Müllen, K.; Gombert, A.; Wittwer, V. A Flexible Conjugated Polymer Laser. *Adv. Mater.* **1998**, *10* (12), 920−923.

(14) Sirringhaus, H.; Tessler, N.; Friend, R. H. Integrated Optoelectronic Devices Based on Conjugated Polymers. *Science* **1998**, *280* (5370), 1741−1744.

(15) Zalar, P.; Pho, T. V.; Garcia, A.; Walker, B.; Walker, W.; Wudl, F.; Nguyen, T. Q. Optical and Charge Transport Properties of Water/Alcohol-Soluble Quinacridone Derivatives for Application in Polymer Light Emitting Diodes. *J. Phys. Chem. C* **2011**, *115* (35), 17533−17539.

(16) Beenken, W. J. D. Excitons in Conjugated Polymers: Do We Need a Paradigma Change? *Phys. Status Solidi A* **2009**, *206* (12), 2750−2756.

(17) Laquai, F.; Park, Y. S.; Kim, J. J.; Basche, T. Excitation Energy Transfer in Organic Materials: From Fundamentals to Optoelectronic Devices. *Macromol. Rapid Commun.* **2009**, *30* (14), 1203−1231.

(18) Hoffmann, S. T.; Bassler, H.; Kohler, A. What Determines Inhomogeneous Broadening of Electronic Transitions in Conjugated Polymers? *J. Phys. Chem. B* **2010**, *114* (51), 17037−17048.
(19) Pina, J.; Costa, T.; Seixas de Melo, J. S. Dynamics and Photophysics of Oligomers and Polymers. In *Specialist Periodic Reports in Photochemistry*; Albini, A., Ed.; RSC: Cambridge, U.K., 2010; Vol. *38*, pp 69−111.
(20) Athanasopoulos, S.; Emelianova, E. V.; Walker, A. B.; Beljonne, D. Exciton Diffusion in Energetically Disordered Organic Materials. *Phys. Rev. B* **2009**, *80* (19), 195209/1−195209/7.
(21) Barford, W.; Trembath, D. Exciton Localization in Polymers with Static Disorder. *Phys. Rev. B* **2009**, *80* (16), 165418.
(22) Zade, S. S.; Zamoshchik, N.; Bendikov, M. From Short Conjugated Oligomers to Conjugated Polymers. Lessons from Studies on Long Conjugated Oligomers. *Acc. Chem. Res.* **2011**, *44* (1), 14−24.
(23) Lupton, J. M.; Pogantsch, A.; Piok, T.; List, E. J. W.; Patil, S.; Scherf, U. Intrinsic Room-Temperature Electrophosphorescence from a Pi-Conjugated Polymer. *Phys. Rev. Lett.* **2002**, *89* (16), 167401.
(24) Westenhoff, S.; Beenken, W. J. D.; Friend, R. H.; Greenham, N. C.; Yartsev, A.; Sundström, V. Anomalous Energy Transfer Dynamics Due to Torsional Relaxation in a Conjugated Polymer. *Phys. Rev. Lett.* **2006**, *97* (16), 166804.
(25) Ferreira, B.; da Silva, P. F.; Seixas de Melo, J. S.; Pina, J.; Maçanita, A. Excited-State Dynamics and Self-Organization of Poly(3-hexylthiophene) (P3HT) in Solution and Thin Films. *J. Phys. Chem. B* **2012**, *116* (8), 2347−2355.
(26) Schwartz, B. J. Conjugated Polymers as Molecular Materials: How Chain Conformation and Film Morphology Influence Energy Transfer and Interchain Interactions. *Annu. Rev. Phys. Chem.* **2003**, *54*, 141−172.
(27) Sartori, S. S.; De Feyter, S.; Hofkens, J.; Van der Auweraer, M.; De Schryver, F.; Brunner, K.; Hofstraat, J. W. Host Matrix Dependence on the Photophysical Properties of Individual Conjugated Polymer Chains. *Macromolecules* **2003**, *36* (2), 500−507.
(28) Mirzov, O.; Bloem, R.; Hania, P. R.; Thomsson, D.; Lin, H. Z.; Scheblykin, I. G. Polarization Portraits of Single Multichromophoric Systems: Visualizing Conformation and Energy Transfer. *Small* **2009**, *5* (16), 1877−1888.
(29) Xie, Y.; Li, Y.; Xiao, L. X.; Qiao, Q. Q.; Dhakal, R.; Zhang, Z. L.; Gong, Q. H.; Galipeau, D.; Yan, X. Z. Femtosecond Time-Resolved Fluorescence Study of P3HT/PCBM Blend Films. *J. Phys. Chem. C* **2010**, *114* (34), 14590−14600.
(30) Simas, E. R.; Gehlen, M. H.; Pinto, M. F. S.; Siqueira, J.; Misoguti, L. Intrachain Energy Migration to Weak Charge-Transfer State in Polyfluorene End-Capped with Naphthalimide Derivative. *J. Phys. Chem. A* **2010**, *114* (47), 12384−12390.
(31) Schmid, S. A.; Abbel, R.; Schenning, A.; Meijer, E. W.; Herz, L. M. Impact of Nuclear Lattice Relaxation on the Excitation Energy Transfer along a Chain of π-Conjugated Molecules. *Phys. Rev. B* **2010**, *81* (8), 085438.
(32) Grell, M.; Knoll, W.; Lupo, D.; Meisel, A.; Miteva, T.; Neher, D.; Nothofer, H. G.; Scherf, U.; Yasuda, A. Blue Polarized Electroluminescence from a Liquid Crystalline Polyfluorene. *Adv. Mater.* **1999**, *11* (8), 671−675.
(33) Fytas, G.; Nothofer, H. G.; Scherf, U.; Vlassopoulos, D.; Meier, G. Structure and Dynamics of Nondilute Polyfluorene Solutions. *Macromolecules* **2002**, *35* (2), 481−488.
(34) Montalti, M.; Credi, A.; Prodi, L.; Gandolfi, M. T. *Handbook of Photochemistry*, 3rd ed.; CRC Press: Boca Raton, FL, 2006.
(35) Pina, J.; Seixas de Melo, J.; Burrows, H. D.; Maçanita, A. L.; Galbrecht, F.; Bunnagel, T.; Scherf, U. Alternating Binaphthyl−Thiophene Copolymers: Synthesis, Spectroscopy, and Photophysics and Their Relevance to the Question of Energy Migration versus Conformational Relaxation. *Macromolecules* **2009**, *42* (5), 1710−1719.
(36) Striker, G.; Subramaniam, V.; Seidel, C. A. M.; Volkmer, A. Photochromicity and Fluorescence Lifetimes of Green Fluorescent Protein. *J. Phys. Chem. B* **1999**, *103*, 8612−8617.
(37) Dias, F. B.; Maçanita, A. L.; Seixas de Melo, J.; Burrows, H. D.; Guntner, R.; Scherf, U.; Monkman, A. P. Picosecond Conformational Relaxation of Singlet Excited Polyfluorene in Solution. *J. Chem. Phys.* **2003**, *118* (15), 7119−7126.
(38) Hintschich, S. I.; Dias, F. B.; Monkman, A. P. Dynamics of Conformational Relaxation in Photoexcited Oligofluorenes and Polyfluorene. *Phys. Rev. B* **2006**, *74* (4), 045210.
(39) Bright, D. W.; Dias, F. B.; Galbrecht, F.; Scherf, U.; Monkman, A. P. The Influence of Alkyl-Chain Length on Beta-Phase Formation in Polyfluorenes. *Adv. Funct. Mater.* **2009**, *19* (1), 67−73.
(40) Teetsov, J.; Fox, M. A. Photophysical Characterization of Dilute Solutions and Ordered Thin Films of Alkyl-Substituted Polyfluorenes. *J. Mater. Chem.* **1999**, *9* (9), 2117−2122.
(41) Anemian, R.; Mulatier, J. C.; Andraud, C.; Stephan, O.; Vial, J. C. Monodisperse Fluorene Oligomers Exhibiting Strong Dipolar Coupling Interactions. *Chem. Commun.* **2002**, *15*, 1608−1609.
(42) Wu, P. L.; Xia, P. F.; Li, Z. H.; Feng, X. J.; Tam, H. L.; Li, K. F.; Jiao, Y.; Wong, M. S.; Cheah, K. W. Non-Coplanar 9,9-Diphenyl-Substituted Oligofluorenes with Large Two-Photon Absorption Enhancement. *Chem. Commun.* **2009**, *36*, 5421−5423.
(43) Geng, Y. H.; Trajkovska, A.; Katsis, D.; Ou, J. J.; Culligan, S. W.; Chen, S. H. Synthesis, Characterization, and Optical Properties of Monodisperse Chiral Oligofluorenes. *J. Am. Chem. Soc.* **2002**, *124* (28), 8337−8347.
(44) Klaerner, G.; Miller, R. D. Polyfluorene Derivatives: Effective Conjugation Lengths from Well-Defined Oligomers. *Macromolecules* **1998**, *31* (6), 2007−2009.
(45) Traiphol, R.; Charoenthai, N.; Manorat, P.; Pattanatornchai, T.; Srikhirin, T.; Kerdcharoen, T.; Osotchan, T. Photophysical Change of Poly(9,9-di(2-ethylhexyl)fluorene) and Its Copolymer with Anthracene in Solvent−Non-Solvent: Roles of Interchain Interactions on the Formation of Non-Emissive and Emissive Aggregates. *Synth. Met.* **2009**, *159* (12), 1224−1233.
(46) Di Paolo, R. E.; Seixas de Melo, J.; Pina, J.; Burrows, H. D.; Morgado, J.; Maçanita, A. L. Conformational Relaxation of *p*-Phenylenevinylene (PV) Trimers in Solution, Studied by Picosecond Time-Resolved Fluorescence. *ChemPhysChem* **2007**, *8*, 2657−2664.
(47) Parkinson, P.; Muller, C.; Stingelin, N.; Johnston, M. B.; Herz, L. M. Role of Ultrafast Torsional Relaxation in the Emission from Polythiophene Aggregates. *J. Phys. Chem. Lett.* **2010**, *1* (19), 2788−2792.
(48) Wells, N. P.; Boudouris, B. W.; Hillmyer, M. A.; Blank, D. A. Intramolecular Exciton Relaxation and Migration Dynamics in Poly(3-hexylthiophene). *J. Phys. Chem. C* **2007**, *111* (42), 15404−15414.
(49) Jespersen, K. G.; Yartsev, A.; Pascher, T.; Sundstrom, V. Excited State Dynamics in Alternating Polyfluorene Copolymers. *Synth. Met.* **2005**, *155* (2), 262−265.
(50) Maçanita, A. L.; Horta, A.; Pierola, I. F. Photophysics of Siloxanes—Influence of Preformed Dimers and Transition from Low-Temperature to High-Temperature Behavior of Dimeric and Polymeric Methylphenylsiloxane. *Macromolecules* **1994**, *27* (4), 958−963.
(51) Seixas de Melo, J.; Costa, T.; Francisco, A.; Maçanita, A. L.; Gago, S.; Gonçalves, I. S. Dynamics of Short As Compared with Long Poly(acrylic acid) Chains Hydrophobically Modified with Pyrene, As Followed by Fluorescence Techniques. *Phys. Chem. Chem. Phys.* **2007**, *9* (11), 1370−1385.
(52) Santos, F. J. V.; de Castro, C. A. N.; Dymond, J. H.; Dalaouti, N. K.; Assael, M. J.; Nagashima, A. Standard Reference Data for the Viscosity of Toluene. *J. Phys. Chem. Ref. Data* **2006**, *35* (1), 1−8.
(53) Gardecki, J. A.; Maroncelli, M. Comparison of the Single-Wavelength and Spectral-Reconstruction Methods for Determining the Solvation-Response Function. *J. Phys. Chem. A* **1999**, *103* (9), 1187−1197.
(54) Reynolds, L.; Gardecki, J. A.; Frankland, S. J. V.; Horng, M. L.; Maroncelli, M. Dipole Solvation in Nondipolar Solvents: Experimental Studies of Reorganization Energies and Solvation Dynamics. *J. Phys. Chem.* **1996**, *100* (24), 10337−10354.
(55) Horng, M. L.; Gardecki, J. A.; Maroncelli, M. Rotational Dynamics of Coumarin 153: Time-Dependent Friction, Dielectric

Friction, and Other Nonhydrodynamic Effects. *J. Phys. Chem. A* **1997**, *101* (6), 1030−1047.
(56) Pina, J.; Burrows, H. D.; Becker, R. S.; Dias, F. B.; Maçanita, A. L.; Seixas de Melo, J. Photophysical Studies of alpha,w-Dicyano-oligothiophenes $NC(C_4H_2S)nCN$ (n = 1−6). *J. Phys. Chem. B* **2006**, *110*, 6499−6505.
(57) Becker, R. S.; Seixas de Melo, J.; Maçanita, A. L.; Elisei, F. Comprehensive Evaluation of the Absorption, Photophysical, Energy Transfer, Structural, and Theoretical Properties of Alpha-Oligothiophenes with One to Seven Rings. *J. Phys. Chem.* **1996**, *100* (48), 18683−18695.
(58) Meng, K.; Liu, Y. L.; Feng, W. K.; Zeng, Q.; Zhao, X. J.; Wang, S. F.; Gong, Q. H. Transient Photophysics of Phenothiazine-Thiophene/Furan Copolymers in Solvents. *J. Photochem. Photobiol., A* **2010**, *210* (1), 44−47.
(59) Galvão, A. M.; Di Paolo, R. E.; Maçanita, A. L.; Naqvi, K. R. Model for Conformational Relaxation of Flexible Conjugated Polymers: Application to *p*-Phenylenevinylene Trimers in Nonpolar Solvents. *ChemPhysChem* **2013**, *14* (3), 583−590.
(60) Maçanita, A. L.; Zachariasse, K. A. Viscosity Dependence of Intramolecular Excimer Formation with 1,5-Bis(1-pyrenylcarboxy)-pentane in Alkane Solvents as a Function of Temperature. *J. Phys. Chem. A* **2011**, *115* (15), 3183−3195.
(61) Di Paolo, R. E.; Gigante, B.; Esteves, M. A.; Pires, N.; Santos, C.; Lameiro, M. H.; Seixas de Melo, J.; Burrows, H. D.; Maçanita, A. L. Picosecond Structural Relaxation of Abietic Acid Based Amine End Capped Para-Phenylenevinylene Trimers in Solution. *ChemPhysChem* **2008**, *9* (15), 2214−2220.
(62) Justino, L. L. G.; Ramos, M. L.; Knaapila, M.; Marques, A. T.; Kudla, C. J.; Scherf, U.; Almasy, L.; Schweins, R.; Burrows, H. D.; Monkman, A. P. Gel Formation and Interpolymer Alkyl Chain Interactions with Poly(9,9-dioctylfluorene-2,7-diyl) (PFO) in Toluene Solution: Results from NMR, SANS, DFT, and Semiempirical Calculations and Their Implications for PFO beta-Phase Formation. *Macromolecules* **2011**, *44* (2), 334−343.